Cold Spring Harbor Perspectives in Biology
www.cshperspectives.org

Cytosolic Ca^{2+} Buffers

Beat Schwaller

Unit of Anatomy, Department of Medicine, University of Fribourg, Route Albert-Gockel 1, CH-1700 Fribourg, Switzerland

Correspondence: beat.schwaller@unifr.ch

"Ca^{2+} buffers," a class of cytosolic Ca^{2+}-binding proteins, act as modulators of short-lived intracellular Ca^{2+} signals; they affect both the temporal and spatial aspects of these transient increases in $[Ca^{2+}]_i$. Examples of Ca^{2+} buffers include parvalbumins (α and β isoforms), calbindin-D9k, calbindin-D28k, and calretinin. Besides their proven Ca^{2+} buffer function, some might additionally have Ca^{2+} sensor functions. Ca^{2+} buffers have to be viewed as one of the components implicated in the precise regulation of Ca^{2+} signaling and Ca^{2+} homeostasis. Each cell is equipped with proteins, including Ca^{2+} channels, transporters, and pumps that, together with the Ca^{2+} buffers, shape the intracellular Ca^{2+} signals. All of these molecules are not only functionally coupled, but their expression is likely to be regulated in a Ca^{2+}-dependent manner to maintain normal Ca^{2+} signaling, even in the absence or malfunctioning of one of the components.

DEFINITION OF A CYTOSOLIC Ca^{2+} BUFFER

Molecules serving as chelators for Ca^{2+} ions must contain negatively charged groups arranged in such a way as to fulfill the necessary geometrical constraints for chemical coordination. Proteins with appropriately spaced acidic side-chain residues (e.g., glutamate, aspartate) and/or backbone carbonyl groups provide the "cage" in which a Ca^{2+} ion may fit in. Evolutionarily well-conserved protein families differing in the way the Ca^{2+} ions are bound include the annexins, the C2-domain proteins, the EF-hand proteins, the pentraxins, the vitamin-K-dependent proteins, and the intraorganellar low-affinity, high-capacity Ca^{2+}-binding proteins; for more details on the structural diversity of EF-hand motifs, see Gifford et al. (2007), and for other Ca^{2+}-binding sites, see Bindreither and Lackner (2009). However, the term Ca^{2+} buffer is applied only to a small subset of cytosolic proteins of the EF-hand family, including parvalbumins (PV; alpha and beta isoforms), calbindin-D9k (CB-D9k), calbindin-D28k (CB-D28k), and calretinin (CR). The majority of EF-hand proteins belong to the group of "Ca^{2+} sensors"; that is, binding of Ca^{2+} ions induces a conformational change, which permits them to interact with specific targets in a Ca^{2+}-regulated manner. The prototypical examples of Ca^{2+} sensors are calmodulin (Chin and Means 2000) and proteins of the S100 family. However, if present at sufficiently high concentrations, Ca^{2+} sensors may also function as Ca^{2+} buffers. Importantly, cytosolic Ca^{2+} buffers do not act as buffers in analogy to chemical buffers such

Editors: Martin D. Bootman, Michael J. Berridge, James W. Putney, and H. Llewelyn Roderick
Additional Perspectives on Calcium Signaling available at www.cshperspectives.org

Advanced Online Article. Cite this article as *Cold Spring Harb Perspect Biol* doi: 10.1101/cshperspect.a004051

as pH buffers. The latter serve to clamp the pH to a predetermined value in such a way that the addition of an acid or a base elicits only a minor change in the pH of the solution. Therefore, the buffering capacity is highest when the pH is close to the pK value of the corresponding acid/base pair. The situation is fundamentally different for the cytosolic Ca^{2+} buffers. Under basal conditions, $[Ca^{2+}]_i$ is in the order of 20–100 nM. Yet, the dissociation constants for Ca^{2+} ($K_{D,Ca}$) of most Ca^{2+} buffers are almost one order of magnitude larger, ≈200 nM–1.5 μM (Table 1). Thus, in a resting cell, Ca^{2+} buffers are at large in their Ca^{2+}-free state, ready to bind Ca^{2+} ions whenever $[Ca^{2+}]_i$ increases. As a result of their specific properties, Ca^{2+}

Table 1. Properties of selected Ca^{2+}-binding proteins (adapted from Schwaller 2009).

	α PV	β PV (OM)	CB-D9k	CB-D28k	CR
Ca^{2+}-binding sites (functional)	3 (2)	3 (2)	2 (2)	6 (4)	6 (5)
Ca^{2+}-specific/ mixed Ca^{2+}/ Mg^{2+} sites	0/2	1/1	2/0	4/0[a]	5/0
$K_{D,Ca}$ (nM)	4–9[b]	Mixed: 42–45[d]	K_{D1} ≈ 200–500[e] K_{D2} ≈ 60–300	high aff. (h)[f] K_{D1} ≈ 180–240	$K_{D(T)}$ 28 μM[g] $K_{D(R)}$ 68 $K_{D(app)}$ 1.4 μM
		Ca^{2+}-specific: 590–780[d]		medium aff. (m) K_{D2} ≈ 410–510	EF5: 36 μM
$K_{D,Mg}$	≈ 30 μM[b]	160–250 μM[d]		714 μM[a]	4.5 mM[h]
$K_{D,Ca(app)}$ (nM) at $[Mg^{2+}]$ of 0.5–1 mM	150–250[c]	230–310[c]			
$k_{on,Ca}$ ($\mu M^{-1}s^{-1}$)	6[b]		up to 1000[i]	h sites ≈ 12[f] m sites ≈ 82	T sites: 1.8[g] R sites: 310 site EF5: 7.3
$k_{on,Mg}$ ($\mu M^{-1}s^{-1}$)	0.1–1[c]				
cooperativity	no[k]	? yes[l]	yes[m]	yes n_H ≈ 1.1–1.2[a]	yes n_H ≈ 1.3–1.9[g]
$D_{Cabuffer}$ (μm^2s^{-1})	37–43[n] ~12			>100[o] ≈ 25	≈ 25[p]

[a]Although considered as Ca^{2+}-specific, at physiological $[Mg^{2+}]_i$, the apparent Ca^{2+} affinity is approximately two-fold lower (Berggard et al. 2002a).

[b](Eberhard and Erne 1994).

[c]$K_{D,Ca}$ and k_{on} for PV are $[Mg^{2+}]$ dependent; calculated values are estimates at $[Mg^{2+}]_i$ 0.6–0.9 mM.

[d](Cox et al. 1990).

[e](Linse et al. 1991).

[f]CB-D28k has high-affinity (h) and medium-affinity (m) sites, the stochiometry h/m is either 2/2 or 3/1 (Nagerl et al. 2000).

[g]For details, see text and Faas et al. (2007).

[h](Stevens and Rogers 1997).

[i]The value represents the diffusion limit, assuming a maximal Ca^{2+} diffusion rate of ≈ 200 μm^2s^{-1} (Martin et al. 1990).

[k]PV has 2 essentially identical Ca^{2+}-binding sites with n_H close to 1.

[l](Yin et al. 2006).

[m](Akke et al. 1991).

[n]The diffusion coefficients $D_{Cabuffer}$ for PV in muscle myoplasm (37 μm^2s^{-1}) (Maughan and Godt 1999) and Purkinje cell dendrites of 43 μm^2s^{-1}; (Schmidt et al. 2003a); smaller values are measured in PC soma and axons (≈12 μm^2s^{-1}); (Schmidt et al. 2007a).

[o]CB-D28k's mobility in PC dendrites is 26 μm^2s^{-1} (Schmidt et al. 2005), clearly slower than in water (Gabso et al. 1997), and also slower than PV in PC dendrites.

[p]Estimation based on the similar size of CB-D28k and CR.

buffers act in different ways to modulate the spatiotemporal aspects of cytosolic Ca^{2+} signals. How a given Ca^{2+} buffer affects intracellular Ca^{2+} signals depends on several parameters, including the intracellular concentration (Intracellular Concentration), the affinity for Ca^{2+} and other metal ions (Metal-binding Affinities), the kinetics of Ca^{2+} binding and release (Metal-binding Kinetics), and the intracellular mobility (Mobility and Interaction with Ligands). When measuring the total Ca^{2+}-buffering capacity (κ_S) of a cell, often the distinction is made between mobile and immobile buffers (Zhou and Neher 1993). The latter ones are defined as molecules capable of binding cytosolic Ca^{2+} that are not washed out when, for example, the plasma membrane is patched with a pipette. Very little is known about the molecular identity of immobile Ca^{2+} buffers, except their relatively low Ca^{2+} affinity; presumably, they are made up of cytosol-exposed stretches of membrane proteins and/or membrane-associated proteins with a rather low affinity for Ca^{2+} ions. Additionally, negatively charged phospholipid headgroups of the inner leaflet of the plasma membrane serve as "weak" Ca^{2+} chelators (McLaughlin et al. 1981). Thus, the slowly mobile or immobile buffers, together with mobile Ca^{2+} buffers, are responsible for the rather slow diffusion of Ca^{2+} ions inside a cell (Mobility and Interaction with Ligands).

IMPORTANT PARAMETERS TO CHARACTERIZE Ca^{2+} BUFFERS

Intracellular Concentration

The difficulty in obtaining reliable values for Ca^{2+}-buffer concentrations is linked to the fact that those cells that strongly express Ca^{2+} buffers are frequently only a subset of cells (often with complex morphologies) within composite tissues; for example, in a subset of neurons in the brain, in specific segments of the kidney nephron, etc. The concentration of PV is as high as 1.5 mM in the superfast swimbladder muscle of toadfish (Tikunov and Rome 2009) and approximately 1 mM in mouse fast-twitch muscle, while it is lower in other muscles and highly correlated with the speed of muscle relaxation (Heizmann et al. 1982). Within different neuron subpopulations, PV is on average one order of magnitude lower (50–150 μM): 80 μM in mouse (Schmidt et al. 2003b) and 120 μM in rat (Hackney et al. 2005) Purkinje cells; 150 μM in mouse cerebellar interneurons (Collin et al. 2005), and 100–300 μM in inner and outer hair cells from inner ear (Hackney et al. 2005). The concentration of mammalian β PV called oncomodulin (OM) is particularly high in rat cochlear outer hair cells (2–3 mM) (Hackney et al. 2005). High concentrations of CR (1.2 mM) are also present in tall saccular hair cells of the frog (Edmonds et al. 2000). In other cells, calretinin concentration is much lower: approximately 20 μM and 35 μM in rat inner and outer hair cells, respectively (Hackney et al. 2005), and 30–40 μM in mouse cerebellar granule cells (Gall et al. 2003). The concentration of CB-D28k is 150–360 μM in Purkinje cells (for a review, see Schwaller et al. 2002), and 40–50 μM in mature hippocampal dentate gyrus granule cells, CA3 interneurons, and in CA1 pyramidal cells (Muller et al. 2005). In cells expressing various mobile and immobile Ca^{2+} buffers of unknown identities and Ca^{2+}-binding properties, the concept of the Ca^{2+}-binding ratio of endogenous buffers has proven to be useful. The ratio of buffer-bound Ca^{2+} changes over free Ca^{2+} changes ($\kappa_S \sim [Ca^{2+}\ \text{buffer}]/K_{D,Ca}$) serves as a measure to compare the Ca^{2+}-buffering capacity of different cell types. According to the single compartment and linear approximation model (Neher 1998), motor neurons with low cytosolic Ca^{2+} buffer expression also have a very low Ca^{2+}-buffering capacity ($\kappa_S < 50$) (Lips and Keller 1998). Hippocampal principal neurons and PV-expressing interneurons have κ_S values in the order of 60 and 150, respectively (Lee et al. 2000b). The highest Ca^{2+}-buffering capacity (κ_S of 900–2000) is seen in cerebellar Purkinje cells expressing high levels of CB-D28k and PV (Fierro and Llano 1996).

Metal-binding Affinities

Structurally, different types of EF-hand domains exist: the canonical EF-hand domain, comprising a Ca^{2+}-binding loop of 12 amino

acids, in which Ca^{2+} ions are mostly coordinated via oxygen atoms of carboxyl side chain groups, and several non-canonical ones (Gifford et al. 2007). Typical for proteins of the S100 family, including CB-D9k (Marenholz et al. 2004), is the presence of a noncanonical loop, termed pseudo (Ψ) EF-hand, consisting of a loop of 14 amino acids with an inside-out conformation compared to the canonical loop; that is, Ca^{2+}-coordination is preferentially provided by backbone carbonyl groups (Nelson et al. 2002). Functionally, two types of EF-hand Ca^{2+}-binding sites are discernable due to their different selectivity and affinity for Ca^{2+} and Mg^{2+} ions (Celio et al. 1996). The Ca^{2+}-specific sites display affinities for Ca^{2+} (K_{Ca}) in the order of 10^{-3}–10^{-7} M and significantly lower ones for Mg^{2+} ($K_{Mg} = 10^{-1}$–10^{-2} M). The proteins CB-D28k and CR have 4 and 5 functional Ca^{2+}-binding sites of this type, respectively. The mixed Ca^{2+}/Mg^{2+} sites bind Ca^{2+} with high and Mg^{2+} with moderate affinity in a competitive manner (dissociation constants: $K_{Ca} = 10^{-7}$–10^{-9} M; $K_{Mg} = 10^{-3}$–10^{-5} M) (Table 1). PV is the prototypical example of a protein with two mixed sites. Based on PV's affinities for Ca^{2+} and Mg^{2+} and with $[Ca^{2+}]_i$ (of approximately 50 nM) and $[Mg^{2+}]_i$ (0.5–1 mM) inside a cell under basal conditions, PV's two Ca^{2+}/Mg^{2+} sites are, to a large degree, occupied by Mg^{2+}. In most proteins, EF-hand domains are paired; two helix-Ca^{2+}-binding loop-helix regions are connected by a short stretch of 5–10 amino acid residues and form a functional unit. Aside from providing structural stability of EF-hand domains, due to the close apposition also of the Ca^{2+}-binding loops in such a tandem domain (Fig. 1), binding of a Ca^{2+} ion to one loop may allosterically affect the other, both with respect to affinity and binding kinetics (Faas et al. 2007; Nelson et al. 2002). As a result of this building principle, the majority of EF-hand proteins have an even number of Ca^{2+}-binding domains (2 in CB-D9k, 6 in CB-D28k and CR); the uneven number (3) for PV (alpha and beta) is, together with the group of penta-EF-hand Ca^{2+}-binding proteins (Maki et al. 2002), rather the exception.

Metal-binding Kinetics

The majority of Ca^{2+} buffers have dissociation constants ($K_{D,Ca}$) in the low micromolar range (Table 1). Thus, in a resting cell (e.g., muscle fibers, neurons), Ca^{2+} buffers are mostly in the Ca^{2+}-free form. It is the kinetics of various Ca^{2+} buffers that strongly affect the spatiotemporal aspects of Ca^{2+} signals, in particular, in excitable cells (Schmidt et al. 2007b; Schmidt and Eilers 2009; Schwaller 2009). $[Ca^{2+}]_i$ transients last for tens of milliseconds to several hundred milliseconds and, thus, are differently modulated by kinetically distinct Ca^{2+} buffers. Their on-rates for Ca^{2+} binding (k_{on}) vary by more than two orders of magnitude. Typical fast buffers with Ca^{2+}-specific sites, including CB-D9k and troponin C, have k_{on} rates $>10^8$ $M^{-1}s^{-1}$ comparable to the on-rate of the synthetic buffer BAPTA. At the other end of the kinetic scale, on-rates for the slow-onset buffer PV are $\approx 3 \times 10^6$ $M^{-1}s^{-1}$ under physiological conditions with $[Mg^{2+}]_i$ of $\approx$0.5–1.0 mM. PV's slow on-rate is the result of PV's Mg^{2+}/Ca^{2+} binding sites, where the rate for Ca^{2+}-binding is determined by the slow Mg^{2+} off-rate (Lee et al. 2000c) (Table 1). Of importance, in a nonphysiological setting, that is, in the absence of Mg^{2+}, the on-rate of Ca^{2+} binding to PV is very rapid (1.08×10^8 $M^{-1}s^{-1}$), almost as fast as the "fast" buffers (Lee et al. 2000c).

Since all endogenous Ca^{2+} buffers have more than one Ca^{2+}-binding site, a given protein may have sites with different affinities and kinetics; results for CB-D28k and CR are summarized here. CB-D28k contains two types of binding sites differing in $K_{D,Ca}$ and k_{on}: One type is a high-affinity site ($K_{D,Ca} \approx 200$ nM) that binds Ca^{2+} with a k_{on} comparable to that of EGTA ($\approx 1 \times 10^7$ M^{-1} s^{-1}), and the second type binds Ca^{2+} with intermediate affinity ($K_{D,Ca} \approx$ 400–500 nM), but with an approximately 8-fold faster k_{on} (Table 1). The ratio between high:intermediate affinity sites is either 3:1 or 2:2. The experimental data could be equally well modeled with either stochiometry for the two types of binding sites (Nagerl et al. 2000). For determining CR's kinetic Ca^{2+}-binding properties in vitro, cooperativity was included

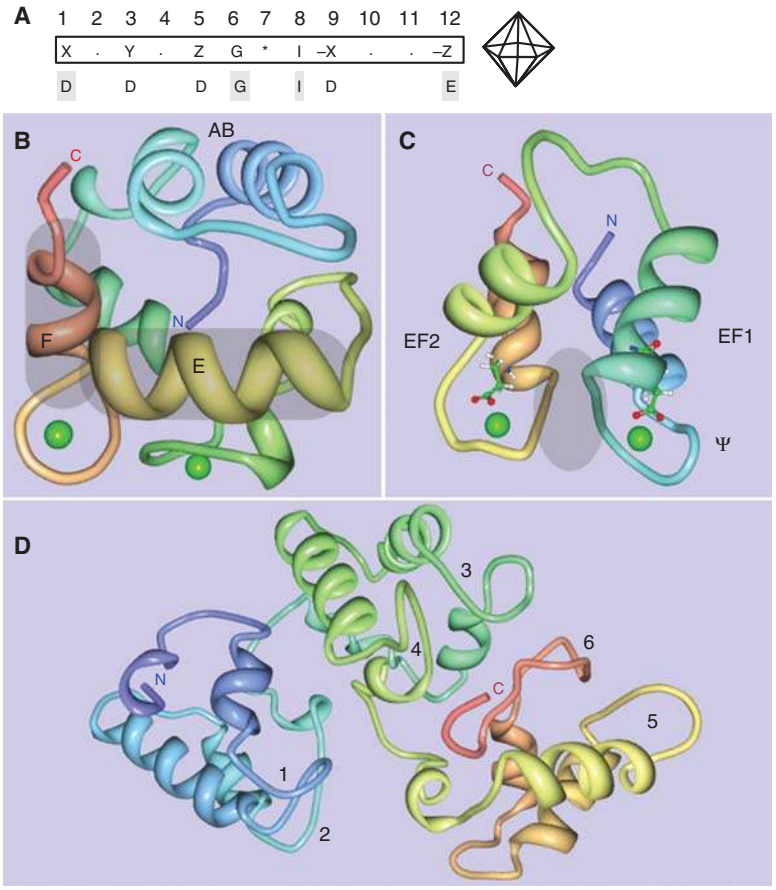

Figure 1. 3D-structures of selected EF-hand Ca^{2+} buffers. (*A*) Consensus sequence of the canonical EF-hand Ca^{2+}-binding loop of 12 amino acids. Amino acids X, Y, Z, and –Z provide side-chain oxygen ligands, * provides the backbone carbonyl oxygen, and at –X, a water molecule is hydrogen-bonded to a loop residue. Amino acids most often present at a given position are shown below, and shaded residues are the most conserved ones (Marsden et al. 1990). At positions X and –Z, Asp (D) and Glu (E) are generally present, respectively. The seven oxygen ligands coordinating the Ca^{2+} ion are located at the seven corners of a pentagonal bipyramid, and the Ca^{2+} ion (not shown) is in the center (right). (*B*) Solution structure of Ca^{2+}-bound human α PV; PDB: 1RJV. Both the CD domain (green) and EF domain (yellow/red) bind one Ca^{2+} ion each (green spheres) in canonical Ca^{2+}-binding loops of 12 amino acids. The orthogonally oriented helices E and F (gray-shaded) are connected by the Ca^{2+}-binding loop. Both Ca^{2+}-binding sites in PV are of the Ca^{2+}/Mg^{2+} mixed type. The N-terminal AB domain (blue) is necessary for protein stability. (*C*) NMR solution structure of bovine CB-D9k; PDB: 1B1G. The shown structure takes into account the Ca^{2+} ions and explicit solvent molecules. The N-terminal domain EF1 is a pseudo (Ψ) EF-hand with a larger loop of 14 amino acids, while the second domain (EF2) has a canonical Ca^{2+}-binding loop of 12 amino acids. In both loops, the Glu residue at the position –Z with the 2 carboxyl oxygen atoms (red) serves as a bidentate ligand representing two corners of the pentagonal bipyramid. This residue, most often Glu (rarely Asp), is a critical determinant for the Ca^{2+} affinity of the entire loop; Ca^{2+} ions are shown as green spheres. The two Ca^{2+}-binding loops are in close proximity and stabilized via short β-type interactions (gray-shaded area). (*D*) 3D NMR structure of CB-D28k; PDB: 2G9B. CB-D28k has a relatively compact structure comprising three Ca^{2+}-binding units, each unit consisting of a pair of EF-hands. Ca^{2+}-binding is restricted to the Ca^{2+}-binding loop 1 in the N-terminal unit (blue), to both loops 3 and 4 in the middle unit (green), and to loop 5 in the C-terminal pair (yellow/red). EF-hands 2 and 6 are nonfunctional, with respect to Ca^{2+}-binding. The Ca^{2+}-binding loops flanked by two almost perpendicular alpha-helical regions are numbered from 1 to 6. Images B–D were generated with PDB ProteinWorkshop 1.50 (Moreland et al. 2005).

in the mathematical model (Table 1). CR contains four 4 high-affinity, cooperative binding sites (Schwaller et al. 1997; Stevens and Rogers 1997) organized into two indistinguishable pairs, probably 1 & 2 and 3 & 4 (Faas et al. 2007) and one independent low-affinity Ca^{2+}-binding site (EF5) with an intrinsic dissociation constant (K'_D) of ≈0.5 mM (Schwaller et al. 1997). Within cooperative pairs, the two binding sites influence each other in an allosteric manner. In a pair, initially both binding sites are in a T- (tense) state, with a low affinity and slow binding rate. When the first Ca^{2+} ion is bound to a pair, the unoccupied site changes to an R- (relaxed) state, characterized by a high affinity and a fast binding rate. This leads to a gradual increase in the Ca^{2+} association rate (k_{on}) as $[Ca^{2+}]_i$ increases from a concentration in a resting neuron (≈50 nM) to approximately 1–10 μM after opening of Ca^{2+} channels (Schwaller 2009). Therefore, the kinetics of Ca^{2+} buffering of CR powerfully depends on the prevailing Ca^{2+} concentration prior to a perturbation, resulting in non-linear Ca^{2+} buffering by CR (for more details, see Fig. 3 in Schwaller 2009 and Faas et al. 2007).

Mobility and Interaction with Ligands

In an aqueous solution, the mobility defined as the diffusion coefficient (D) of a molecule is approximately proportional to the hydrodynamic radius (i.e., approximately proportional to the relative molecular mass; M_r). For relatively large molecules, such as dextrans and globular proteins, D should be proportional to the inverse cubic root of M_r. In Purkinje cells, PV is freely mobile, but D can vary considerably in different compartments: ≈12 $\mu m^2/s$ in axons, somata, and nuclei (Schmidt et al. 2007a) versus ≈43 $\mu m^2/s$ in dendrites (Schmidt et al. 2003a), most likely as the result of different cytoplasmic properties (e.g., tortuosity; i.e., diffusion in a porous medium). The latter value is very similar to PV's mobility in frog myoplasm, 43 and 32 $\mu m^2/s$ for transverse and longitudinal diffusion, respectively (Maughan and Godt 1999), but clearly smaller than in an aqueous solution: 140 $\mu m^2/s$ (Feher 1984). As expected from the larger M_r of CB-D28k (≈29 kDa) compared to PV (≈12 kDa), D in Purkinje cell dendrites is smaller: 26 $\mu m^2/s$ (Schmidt et al. 2005). How the presence of a Ca^{2+} buffer affects the spatiotemporal aspects of a cytosolic Ca^{2+} transient not only depends on the mobility of the Ca^{2+} buffer, but also on the mobility of the free Ca^{2+} ions. In the cytosol isolated from *Xenopus laevis* oocytes, the diffusion coefficient D of inositol 1,4,5-trisphophate ($InsP_3$) is much bigger than that of Ca^{2+} ions in a solution with $[Ca^{2+}]_i$ of 90 nM: 283 $\mu m^2/s$ versus 13 $\mu m^2/s$, respectively (Allbritton et al. 1992). Even when $[Ca^{2+}]_i$ is increased to 1 μM, presumably saturating slowly mobile and immobile buffers, D_{Ca} only reaches a value of 65 $\mu m^2/s$. This indicates that the slow diffusion of Ca^{2+} ions in a resting cell ($[Ca^{2+}]_i \approx 50$ nM) is caused by slowly mobile or immobile buffers "acting like velcro" for Ca^{2+} ions, limiting the effective range of an unbuffered free Ca^{2+} ion to ≈0.1 μm. Thus, the range of Ca^{2+} can be increased by buffered diffusion, that is, mobile Ca^{2+} buffers acting as shuttles transporting Ca^{2+} through the "mesh of immobile buffers" (Schmidt et al. 2007b).

Parvalbumins

Structural Aspects of Parvalbumins

The first prototypical structure of an EF-hand domain was determined in PV (Kretsinger and Nockolds 1973), an atypical EF-hand protein; the protein ($M_r \approx 12$ kDa; human gene symbol: *PVALB*) has an uneven number (3) of EF-hand domains, and the Ca^{2+} -binding sites are Ca^{2+}/Mg^{2+} mixed sites (Table 1). While the two C-terminal domains CD and EF are functional metal-binding sites, the N-terminal AB site is necessary for the PV's stability (Fig. 1) (Cox et al. (1999). The CD and EF domains form a pair consisting of two helix-loop-helix regions linked by a short stretch of 5–10 amino acid residues. In both sites, the Ca^{2+} ion in the center of the loop is coordinated by seven ligands sitting in the corners of a pentagonal bipyramid (Swain et al. 1989). Results based on solution structures of α PV and β PV (Babini et al. 2004) in the Ca^{2+}-loaded and the apo (metal-free) form

are summarized: (I) PV's Ca^{2+}-loaded EF-hand domains and the linker region connecting the CD and EF domains are rather rigid structures; also the N- and C-termini of PV have a low intrinsic mobility (Baldellon et al. 1998); (II) Differences in the structure of apo- and Ca^{2+}-loaded forms of rat PV are small, mostly confined to the loop region. Thus, Ca^{2+} binding does not require major structural rearrangements (Henzl and Tanner 2008); (III) The first two points also hold true for the Ca^{2+}/Mg^{2+} (EF) site in rat β PV, while the noncanonical CD site undergoes significant structural alterations, when Ca^{2+} is removed from β PV (Henzl and Tanner 2007). Thus, the global rigidity of α PV favors this molecule to serve as a "simple" Ca^{2+} buffer, while the Ca^{2+}-dependent conformational changes in β PV may provide β PV also with a Ca^{2+} sensor function.

Functional Aspects of Parvalbumin and Oncomodulin

Cells with high PV expression levels include a subset of mostly GABA-ergic neurons, fast-twitch muscle fibers, and epithelial cells in the early distal convoluted tubule (DCT1) in nephrons of the kidney. PV's slow-onset Ca^{2+}-binding properties affect Ca^{2+} transients in a particular way: The rate in rise in $[Ca^{2+}]_i$ is hardly affected, but the initial rate of $[Ca^{2+}]_i$ decay is increased. In the later phase of the decay, the unbinding of Ca^{2+} ions from PV prolongs the late phase of the $[Ca^{2+}]_i$ decay. Thus, PV's hallmark is the conversion of a monoexponential $[Ca^{2+}]_i$ decay into a biexponential one (Collin et al. 2005; Lee et al. 2000c). In fast-twitch muscles, this increases muscle relaxation of an electrically induced muscle twitch, while barely affecting the contraction phase. In PV knockout mice ($PV^{-/-}$), twitch half-relaxation rates in fast muscles are slower than in the PV-expressing wild-type (WT) muscles (Schwaller et al. 1999). Conversely, the overexpression of PV by injection of *Pvalb* cDNA into the rat slow-twitch muscle, soleus, significantly increases the speed of relaxation, without affecting the contraction (Muntener et al. 1995). *Pvalb* gene delivery in rat heart in vivo increases the rate of heart relaxation in normal hearts and in an animal model of slowed cardiac muscle relaxation (Szatkowski et al. 2001). Thus, PV or genetically "tuned" PV variants are discussed as potential tools to enhance cardiac diastolic function (Rodenbaugh et al. 2007; Wang and Metzger 2008). An often-neglected aspect is the role of Ca^{2+} buffers in acting as transient Ca^{2+} sources, prolonging the $[Ca^{2+}]_i$ decay. In fast-twitch muscles subjected to long tetanic contractions, PV saturates with Ca^{2+} and consequently slows down relaxation (Raymackers et al. 2000). The slow decay component mediated by Ca^{2+}-bound PV also leads to a robust, PV-dependent, delayed transmitter release at cerebellar interneuron–interneuron synapses subsequent to presynaptic bursts of action potentials (Collin et al. 2005).

The PV-mediated, biexponential $[Ca^{2+}]_i$ decay is observed in: (I) PV-injected chromaffin cells (Lee et al. 2000c); (II) PV-containing hippocampal interneurons (Lee et al. 2000b); (III) PV-expressing molecular layer interneurons (MLI) in the cerebellum (Collin et al. 2005); (IV) presynaptic terminals of the calyx of Held (Muller et al. 2007); and (V) in Purkinje cell dendrites (Schmidt et al. 2007a). PV's acceleration of the early phase of $[Ca^{2+}]_i$ decay limits or slows down the buildup of residual $[Ca^{2+}]_i$ in presynaptic terminals, thus affecting short-term plasticity. The effect is most pronounced at timepoints, when $[Ca^{2+}]_i$ decay curves in the presence or absence of PV show the largest differences. PV's effect on decreasing/preventing paired-pulse facilitation at synapses between MLI and Purkinje cells is most pronounced at ≈33 Hz (Caillard et al. 2000). Also in the presynaptic terminals of the calyx of Held, PV accelerates the decay of spatially averaged $[Ca^{2+}]_i$ and paired-pulse facilitation (Muller et al. 2007). In hippocampal PV-interneurons, differences in paired-pulse modulation between WT and $PV^{-/-}$ mice are apparent only when trains at 33, 50, and 100 Hz are delivered (Vreugdenhil et al. 2003), likely due to differences in components of the Ca^{2+} signaling toolkit and/or more efficient presynaptic Ca^{2+} extrusion mechanisms. The largest relative effect of PV in preventing facilitation is seen at approximately

33 Hz, within the range of gamma frequency (30–80 Hz) oscillations. As a result, the power of kainite-induced gamma oscillations in area CA3 in vitro is approximately 3-fold higher in $PV^{-/-}$ versus WT tissue. This can be explained by an increased facilitation of GABA release at persistent high frequencies. In accordance with the hypothesis that changes in the inhibitory activity of PV neurons in the neocortex—often critically involved in strong perisomatic inhibition—may be a major mechanism underlying epileptic seizures (Mihaly et al. 1997). $PV^{-/-}$ mice have a lower threshold for pentylenetetrazole (PTZ)-induced seizures (Schwaller et al. 2004). The subpopulation of PV-immunoreactive (PV-ir) neurons is critically involved in controlling the output of principal neurons (Freund 2003); moreover, PV is not only a marker for these GABA-ergic interneurons, but contributes to controlling the network activity. The absence of PV in the cerebellar circuitry leads to the emergence of 160-Hz oscillations in vivo sustained by synchronous, rhythmic-firing Purkinje cells aligned along the parallel fiber axis (Servais et al. 2005). Also, $PV^{-/-}$ Purkinje cell-firing properties are different from WT ones: The complex spike duration and the spike pause are decreased, and the simple spike-firing rate is increased. These differences in firing properties, together with the oscillations, are the likely cause for the mild locomotor phenotype, that is, a slight impairment of motor coordination/motor learning (Farre-Castany et al. 2007).

Much less is known about OM's specific function. OM is present in the organ of Corti (Thalmann et al. 1995), more precisely in cochlear outer hair cells (Sakaguchi et al. 1998) in gerbil, rat, and mouse. An extracellular role for OM in retinal ganglion cell regeneration (Yin et al. 2006) was reported, but see also Hauk et al. (2008) and Schwaller (2009). An up-regulation of OM occurs in $PV^{-/-}$ mice in a sparse subpopulation of neurons in the thalamus and in the dentate gyrus, as well as in partly varicose axons in the diencephalon (Csillik et al. 2010). The functional significance of ectopic OM expression and the exact identity of neurons expressing OM in $PV^{-/-}$ mice remain to be shown.

Structural and Functional Aspects of Calbindin-D9k

CB-D9k (human gene symbol: *S100G*) is the smallest protein with four alpha-helical regions forming an EF-hand pair consisting of a canonical (EF2) and a noncanonical/pseudo (EF1) EF-hand domain, joined by a linker region of 10 amino acids (Fig. 1). The tandem domain is stabilized by a short beta-type interaction between the two Ca^{2+}-binding loops (Kordel et al. 1993). The Ca^{2+}-binding affinities of individual subdomains are several orders of magnitude lower than for the corresponding sites within the intact protein. Thus, EF-hands organized in tandem domains are the physiological relevant structures (Finn et al. 1992; Nelson et al. 2002). $K_{D,Ca}$ values are almost identical for both sites (Table 1), and the two Ca^{2+} ions bind with positive cooperativity (Linse et al. 1991). CB-D9k undergoes Ca^{2+}-induced conformational changes; they are, however, less pronounced than in the prototypical sensor calmodulin. This, together with no identified binding partners, indicates that CB-D9k most likely functions as a Ca^{2+} buffer, rather than a Ca^{2+} sensor (Skelton et al. 1994).

In a rat kidney, CB-D9k is expressed in the loop of Henle, the distal convoluted tubule, and in intercalated cells of the collecting duct (Bindels et al. 1991a). In a mouse, CB-D9k expression is present in late distal convoluted tubules (Lee et al. 2006) and the connecting tubules. Strong expression of CB-D9k is restricted to the first 2 cm of the duodenum (Huybers et al. 2007). CB-D9k is assumed to be a freely mobile molecule in the cytoplasm of specific epithelial cells of the kidney and duodenum. Its Ca^{2+}-binding properties, the regulation by $1,25(OH)_2$ vitamin D3 in the intestine, and CB-D9k's relative electrophoretic mobility led to the name calbindin-D9k (Kallfelz et al. 1967). In other tissues, CB-D9k expression is regulated also in other ways (Choi and Jeung 2008), for example, by estrogen in the uterus (Darwish et al. 1991) or by PTH in mouse primary renal tubular cells (Cao et al. 2002). Suggested functions of CB-D9k include a role in the regulation of Ca^{2+} transport processes

across epithelial cells (Bindels et al. 1991b), but also as a Ca^{2+} buffer/shuttle optimally tuned for transcellular Ca^{2+} transport (Choi and Jeung 2008).

Calbindin-D28k

Structural and General Aspects of CB-D28k

CB-D28k ($M_r \approx 29$ kDa; human gene symbol: *CALB1*) has six EF-hand domains, four of which bind Ca^{2+} with medium/high affinity (Cheung et al. 1993). EF-hand 2 is nonfunctional and under physiological conditions EF6 most likely is as well. The four medium/high affinity sites (Nagerl et al. 2000) are considered Ca^{2+}-specific, albeit low affinity Mg^{2+} binding ($K_{D,Mg} \approx 700$ μM) to the same sites at physiological $[Mg^{2+}]_i$ decreases the apparent Ca^{2+} affinity approximately two-fold; additionally, Mg^{2+} binding increases the cooperativity of Ca^{2+} binding (Berggard et al. 2002a). The NMR solution structure of Ca^{2+}-bound rat CB-D28k reveals that it consists of a single, almost globular (ellipsoid) fold with six distinguishable EF-hand domains (Kojetin et al. 2006) (Fig. 1). The on-rates of CB-D28k's fast binding sites ($k_{on} \approx 8. \times 10^7\ M^{-1}s^{-1}$) are fast enough to affect the early rising phase of Ca^{2+} transients; the peak amplitude is significantly decreased in WT Purkinje cells, when compared to Purkinje cells from CB-D28k$^{-/-}$ mice (Airaksinen et al. 1997). The fact that the time to peak is not significantly different in CB-D28k$^{-/-}$ and WT Purkinje cells indicates that the initial rise in $[Ca^{2+}]_i$ is principally governed by the properties (density, kinetics) of the Ca^{2+} channels. In Purkinje cell dendrites, CB-D28k acts as a fast Ca^{2+} buffer for the first approximately 100 ms, reducing the peak $[Ca^{2+}]_i$ amplitude to about one half, while later on prolonging the decay by acting as a Ca^{2+} source (Schmidt et al. 2003b).

Although principally considered as a freely mobile protein, CB-D28k binds to several identified target proteins including Ran-binding protein (RanBP) M (Lutz et al. 2003); caspase-3 (Bellido et al. 2000); 3′,5′-cyclic nucleotide phosphodiesterase (Reisner et al. 1992); plasma membrane ATPase (Morgan et al. 1986); L-type Ca^{2+} channel α subunit (*CANAC1C*) (Christakos et al. 2007); *myo*-inositol monophosphatase (IMPase) (Berggard et al. 2002b); and in the kidney to TRPV5 (Lambers et al. 2006). In most cases, binding studies were performed in vitro; the physiological implications of these interactions are not clear yet. In dendrites and spines of Purkinje cells, approximately 20% of CB-D28k molecules are temporarily, that is, for several seconds, immobile by their binding to IMPase, a key enzyme of the $InsP_3$-signaling cascade, and the fraction of immobilized CB-D28k increases by climbing fiber stimulation (Schmidt et al. 2005). In summary, the above findings, together with CB-D28k's Ca^{2+}-dependent conformational changes, indicate additional Ca^{2+} sensor functions (Berggard et al. 2002a).

Functional Aspects of CB-D28k

Reported functions for CB-D28k include a role in Ca^{2+} resorption in the kidney (Boros et al. 2009) and modulation of insulin production and secretion in pancreatic beta cells (Reddy et al. 1997; Sooy et al. 1999). Data on a putative neuroprotective role against excitotoxicity have not yet resulted in a consistent picture (for a review, see Schwaller et al. 2002 and Schwaller 2009). Results obtained in CB-D28k$^{-/-}$ mice are summarized. At first glance, these mice show no phenotype related to development, the general morphology of the nervous system, the visual (Wassle et al. 1998) and auditory (Airaksinen et al. 2000) systems, or behavior under standard housing conditions (Airaksinen et al. 1997). CB-D28k$^{-/-}$ mice show a mild—however more severe than PV$^{-/-}$ mice—impairment in motor coordination/motor learning (Airaksinen et al. 1997; Farre-Castany et al. 2007), likely resulting from the 160-Hz oscillations in the cerebellum (Cheron et al. 2004; Servais et al. 2005). The motor coordination phenotype is due to CB-D28k's absence in Purkinje cells, since this phenotype and alterations in Purkinje cell physiology also occur in mice with Purkinje cell-specific *Calb1* ablation (Barski et al. 2003). At the cellular level, short-term plasticity between cortical multipolar bursting cells and pyramidal cells, or at the

mossy fiber-CA3 pyramidal cell synapse in the hippocampus, is affected by CB-D28k (Blatow et al. 2003). The rapid saturation of presynaptic CB-D28k transiently decreases the Ca^{2+} buffering capacity, leading to enhanced facilitation (Blatow et al. 2003) by a mechanism called "facilitation by buffer saturation" (Maeda et al. 1999; Neher 1998). Ca^{2+} buffers, such as CB-D28k, also affect Ca^{2+}-dependent inactivation (CDI) of voltage-dependent Ca^{2+} currents (I_{Ca}). In dentate gyrus granule cells with low or absent CB-D28k expression resulting from Ammon's horn sclerosis in humans (AHS) (Nagerl and Mody 1998) or in mice with *Calb1* gene ablation (Klapstein et al. 1998), CDI is increased, compared to CB-D28k-expressing granule cells, thereby decreasing the total Ca^{2+} load. Increased CDI in the absence of CB-D28k may be viewed as a protective/homeostatic mechanism to limit Ca^{2+} influx in order to augment the resistance against excitotoxicity and to protect the surviving neurons.

Structural and Functional Aspects of Calretinin

Human calretinin ($M_r \approx 31$ kDa; gene symbol: *CALB2*) consists of 271 amino acids and has 6 EF-hand domains, five of which are able to bind Ca^{2+} ions (Schwaller et al. 1997; Stevens and Rogers 1997). Structural data (NMR) is available only for the N-terminal 100 amino acids of rat CR comprising EF-hand domains 1 and 2 (Palczewska et al. 2001). As in CB-D28k, the two domains form a relatively tight structure. CR's Ca^{2+}-dependent conformational changes, together with results from other in vitro studies, suggest that CR also may have Ca^{2+}-sensor functions (Billing-Marczak and Kuznicki 1999).

A role for CR in neuroprotection against glutamate toxicity was postulated, but evidence is most often indirect or obtained in model systems in vitro (D'Orlando et al. 2001; Lukas and Jones 1994; Pike and Cotman 1995). For more details, see Schwaller 2009. $CR^{-/-}$ mice show impaired long-term potentiation (LTP) in the hippocampus (Gurden et al. 1998; Schurmans et al. 1997). While the effect on hippocampal LTP is indirect, the uniform expression of CR in cerebellar granule cells, together with the stereotypic cerebellar organization, has allowed for a detailed investigation of CR in vivo. In $CR^{-/-}$ granule cells, the excitability is increased, they show faster action potentials, and, under conditions generating repetitive spike discharges, show enhanced increases in frequency with injected currents (Gall et al. 2003). This leads to altered Ca^{2+} homeostasis in Purkinje cells. The firing properties of Purkinje cells are altered in alert $CR^{-/-}$ mice: The simple spike-firing rate increased the complex spike duration and the spike pause is shorter (Schiffmann et al. 1999). As in $PV^{-/-}$ and $CB\text{-}D28k^{-/-}$ mice, alert $CR^{-/-}$ mice show 160 Hz oscillations (Cheron et al. 2004) that appear phenotypically as an impairment of motor coordination. In alert "rescue" mice, where CR in $CR^{-/-}$ mice is selectively re-expressed in granule cells, granule cell excitability, as well as Purkinje cell firing, resembles that in WT mice. As a consequence, neither 160-Hz oscillations, nor motor coordination impairment, are detected in the rescue mice (Bearzatto et al. 2006).

The similarity of the oscillations and motor coordination deficits in mice deficient for either one of the three CaBPs points toward an effect at the cerebellar network level. In all three knockout strains, the oscillations are temporarily reduced by blocking of: (I) gap junctions between interneurons; (II) N-methyl-D-aspartate receptors; or (III) $GABA_A$ receptors. This indicates that oscillations emerge via a mechanism that synchronizes assemblies of Purkinje cells (mediated by parallel fiber excitation) and the network of chemically-coupled MLI. In addition, recurrent Purkinje cell collaterals (Orduz and Llano 2007) may be implicated in these oscillations (de Solages et al. 2008).

COMPARISON OF THE PHYSIOLOGICAL EFFECTS BROUGHT ABOUT BY CYTOSOLIC Ca^{2+} BUFFERS AND IMMOBILE "Ca^{2+} BUFFERS/STORES", IN PARTICULAR BY MITOCHONDRIA

Cytosolic Ca^{2+} buffers may be viewed as transitory Ca^{2+} sinks/stores, and together with the plasmalemmal extrusion systems, Ca^{2+} uptake

into ER compartments and mitochondria serve as a cell's Ca^{2+} "off mechanisms"; Ca^{2+}-loaded buffers, together with release from Ca^{2+}-filled organelles (ER, mitochondria), subserve as the intracellular "on mechanisms" (Berridge et al. 2003). Here, I briefly put side-by-side the role of mitochondria in Ca^{2+} buffering/sequestration with the role of mobile cytosolic Ca^{2+} buffers. The comparison is primarily focused on excitable cells, mostly neurons (for a more detailed role on mitochondria and Ca^{2+} signaling, see Rimessi et al. 2008 and Szabadkai and Duchen 2008). In the large glutamatergic presynaptic terminals of the calyx of Held, mitochondria contribute to increase the rate in $[Ca^{2+}]_i$ decay, when peak $[Ca^{2+}]_i$ is >2.5 μM (Kim et al. 2005). This mitochondria-mediated increase in $[Ca^{2+}]_i$ decay closely resembles the action of the "slow buffer" PV in the same terminals (Muller et al. 2007). At the physiological level, this delayed buffering by PV and mitochondria affects plasticity of synaptic transmission. More importantly, it has an effect on both short-term facilitation and short-term depression. Blocking mitochondrial Ca^{2+} uptake in the calyx of Held slows down the recovery from synaptic depression (Billups and Forsythe 2002), an effect that can be reverted by the addition of 1 mM EGTA. Slow release of mitochondrial Ca^{2+}, but not from ER stores, leads to the post-tetanic potentiation (PTP) in motor axons contacting the opener muscle of the crayfish *Procambarus clarkii* leg (Tang and Zucker 1997). In analogy, at synapses between molecular layer interneurons (MLI), release of Ca^{2+}, likely from Ca^{2+}-bound PV, increases delayed transmitter release after an AP train (Collin et al. 2005). Both PV and mitochondria hardly affect basal synaptic transmission and show similar effects with respect to short-term modulation. The increased removal of intracellular Ca^{2+} by PV prevents the buildup of residual $[Ca^{2+}]$ and thus reduces paired-pulse facilitation at the calyx of Held and in MLI axon terminals; these findings were deduced by comparing $PV^{-/-}$ and WT mice (Collin et al. 2005; Muller et al. 2007). The reduced density of mitochondria in presynaptic axon terminals of synaptophilin knockout mice ($snph^{-/-}$) affects short-term facilitation in cultured $snph^{-/-}$ hippocampal neurons. While basal synaptic transmission evidenced by single EPSCs and miniature AMPA currents is unaltered, facilitation is increased (Kang et al. 2008). This effect closely resembles the one observed at hippocampal interneuron/CA1 pyramidal neuron synapses in $PV^{-/-}$ mice, where facilitation of IPSCs is augmented at stimulation frequencies >33 Hz (Vreugdenhil et al. 2003).

Both mitochondria and cytosolic Ca^{2+} buffers have an effect on the spreading of intracellular Ca^{2+} waves. While in *Xenopus laevis* oocytes, energized mitochondria promote the propagation of Ca^{2+} waves (Boitier et al. 1999), mitochondria in astrocytes limit the rate and extent of Ca^{2+} wave propagation (Jouaville et al. 1995). Also, Ca^{2+} buffers affect Ca^{2+} waves. The fast buffer CR promotes the spreading of $InsP_3$-evoked Ca^{2+} signals in oocytes, while the slow buffer PV shortens the duration of these Ca^{2+} signals and restricts the global responses to discrete localized events (puffs) (Dargan et al. 2004). In summary: (I) Both mitochondria and cytosolic Ca^{2+} buffers participate in the shaping of Ca^{2+} signals in presynaptic terminals and consequently have an effect on short-term modulation of synaptic plasticity, that is, facilitation, potentiation, and depression; (II) They also affect the spreading of Ca^{2+} waves; the effect depends on the cell type, on the kinetic properties of the cytosolic Ca^{2+} buffers, and also on ER luminal regulatory mechanisms involving the luminal Ca^{2+}-binding protein calreticulin (Camacho and Lechleiter 1995); (III) In the systems investigated so far, PV and mitochondria mostly behave as slow-onset buffers, rarely affecting the maximal amplitude of Ca^{2+} signals, but increasing the rate of $[Ca^{2+}]_i$ decay. In presynaptic terminals, the time window most strongly affected by the Ca^{2+} buffering action of PV and mitochondria is $\approx 10-200$ ms after peak $[Ca^{2+}]_I$; (IV) The physiological effect of Ca^{2+} buffering/sequestering by mitochondria and Ca^{2+} buffers is dependent on the cell type, morphology of involved compartments (e.g., presynaptic terminal, soma) and, importantly, the contribution of all other components from the Ca^{2+}

signaling toolkit; (V) Evidently, PV and mitochondria cannot completely replace one another with respect to Ca^{2+} buffering. They are still different with respect to several parameters: mobility, Ca^{2+} storing capacity, effects of Ca^{2+} binding/uptake on metabolism, Mg^{2+} effects, kinetics of Ca^{2+} binding/release, kinetics of synthesis/degradation, etc. The finding that mitochondria volume and PV expression levels are inversely correlated in several systems is discussed later in this article.

THE Ca^{2+} HOMEOSTASOME

How can a simple change in $[Ca^{2+}]_i$ observed in, for example, muscle contraction, neurotransmission, or cell cycle regulation be used by cells to elicit the correct downstream events, as diverse as membrane fusion of neurosecretory vesicles with the plasma membrane or activation/repression of genes? The obvious parameters are the amplitude of the Ca^{2+} signal and the duration or the frequency at which these signals are generated. Subtler regulations comprise the cell morphology, where Ca^{2+} signals are restricted to certain regions: dendrites, soma, or axon terminals of nerve cells. Finally, molecules implicated in Ca^{2+} signaling may be spatially restricted; for example, Ca^{2+} channel subunits in active zones (Bucurenciu et al. 2008). To achieve the necessary precision of Ca^{2+} signals, cells require an accurately tunable system for regulating $[Ca^{2+}]_i$. Opening of plasma membrane Ca^{2+} channels or Ca^{2+} release from internal stores results in an initial increase in $[Ca^{2+}]_i$. The shape of the Ca^{2+} signal in the cytosol, both with respect to space and time, is then modulated by immobile and, if present, by mobile Ca^{2+} buffers. Finally, extrusion systems such as plasma membrane Ca^{2+} pumps (PMCA), the Na^+/Ca^{2+} exchanger (NCX), and organellar uptake by the ER and/or mitochondria restore the initial situation with respect to $[Ca^{2+}]_i$. All of the above components are part of a cell's "Ca^{2+}-signaling toolkit" that is able to regulate the expression of its own components necessary for accurate and cell-specific Ca^{2+} signaling (Berridge et al. 2003; Schwaller 2009). One of the gene regulators is Ca^{2+} itself, and effects are mediated by Ca^{2+}/calmodulin-dependent kinases (CaMK) and Ca^{2+}-regulated phosphatases (e.g., calcineurin). As an example, long-term survival of cultured cerebellar granule cells is dependent on accurate Ca^{2+} signals necessitating temporal changes in the transcription of Ca^{2+}-signaling toolkit components: IP_3R and PMCAs 2 and 3 are up-regulated, while a PMCA4 splice variant and plasma membrane NCX2 are down-regulated in a calcineurin-dependent manner (Carafoli et al. 1999). Such adaptative/homeostatic mechanisms are also induced if Ca^{2+}-signaling toolkit components are functionally compromised (e.g., in genetic diseases) or purposely eliminated in knockout mice. The network of molecules implicated in Ca^{2+} signaling, homeostasis, and its own regulation is termed the Ca^{2+} homeostasome (Schwaller 2007, 2009).

Results on the modulation of the Ca^{2+} homeostasome brought about by altered expression of CaBPs (e.g., in transgenic mice) are summarized. The most surprising finding is that in essentially all CaBP knockout mice and in a given cell type, the deleted CaBP is not compensated by up-regulating expression of one of the more than 240 other EF-hand family members. That is, in the subset of identified "PV-ergic" neurons (e.g., Purkinje cells, stellate, and basket cells in the cerebellum), none of the other Ca^{2+} buffers (CB-D28k, CB-D9k, or CR) are expressed in the above-mentioned neuron subtypes of $PV^{-/-}$ mice (Schwaller et al. 2004). The same holds true for CR-immunoreactive or CB-D28k-immunoreactive neurons in the respective knockout strains, CB-$D28k^{-/-}$ and $CR^{-/-}$ (Airaksinen et al. 1997; Schiffmann et al. 1999). The most notable exception is the up-regulation of CB-D9k in epithelial kidney cells in CB-$D28k^{-/-}$ mice (Zheng et al. 2004). Two plausible explanations for the absence of compensation/homeostatic mechanisms at the level of other Ca^{2+} buffers are presented: (I) Neurons once committed to express a certain Ca^{2+} buffer have permanently inactivated/repressed the promoter for other Ca^{2+} buffers; (II) The specific properties (affinities, kinetics, cooperativity, mobility) of any other Ca^{2+} buffer would not be adequate to

restore "normal" Ca^{2+} signaling (Schwaller 2009). Thus, if not at the level of other Ca^{2+} buffers, how do cells cope with the absence of a particular Ca^{2+} buffer? Also, does the absence or impairment of other components of the Ca^{2+}-signaling toolkit affect the expression of Ca^{2+} buffers?

Purkinje cells are characterized by extensive Ca^{2+} signaling and high expression levels of PV and CB-D28k and, thus, are well-suited to address these questions. The two Ca^{2+} buffers are present in the soma, axon, dendrites, and spines, indicating that they are principally mobile proteins. While PV is freely mobile in all compartments (Schmidt et al. 2007a), a fraction of CB-D28k molecules is immobilized in dendrites and spines by its binding to IMPase (Schmidt et al. 2005). The most striking alterations in the absence of PV are the morphological changes observed in the soma. The volume of mitochondria, Ca^{2+} sequestrating organelles that also serve as transient Ca^{2+} stores (Billups and Forsythe 2002; Murchison and Griffith 2000), is increased by about 40% selectively in a narrow compartment underneath the plasma membrane (Chen et al. 2006). Concomitantly, the subplasmalemmal smooth ER compartment is decreased (Fig. 2). These changes in the soma don't occur in CB-D28k$^{-/-}$ Purkinje cells. In the latter, subtle changes in the spine morphology are evident: Spines are longer and spine head volume is increased (Vecellio et al. 2000). In spiny pyramidal cells, spine heads are considered as separate biochemical compartments with negligible Ca^{2+} diffusion via the spine neck (Sabatini et al. 2002). However, modeling studies in Purkinje cell spines have revealed that Ca^{2+} buffers are not only involved in modulating the shape of Ca^{2+} transients within the spines, but together with the spine neck geometry also define the amount of Ca^{2+} ions that may reach the parental dendrite and lead to activation of Ca^{2+}-/CaM-dependent signaling cascades (Schmidt and Eilers 2009). Of the two principal Purkinje cell Ca^{2+} buffers, mostly CB-D28k is involved in spino-dendritic coupling by buffered Ca^{2+} diffusion, while the contribution of PV is minute. This is a likely explanation for the unaltered PV$^{-/-}$ Purkinje cell spine morphology. The absence of CB-D28k and PV not only affects Purkinje cell morphology, but also components directly involved in Ca^{2+} signaling. $Ca_v2.1$ (P/Q type) channels are the major voltage-operated Ca^{2+} channels of mature Purkinje cells (>90% of the whole-cell voltage-gated Ca^{2+} current) and regulate Ca^{2+} signaling and excitability of these cells. These channels are regulated by Ca^{2+}-dependent feedback mechanisms consisting of both Ca^{2+}-dependent facilitation (CDF) and inactivation (CDI). While the former process is essentially mediated by the Ca^{2+} sensor calmodulin (CaM) (Lee et al. 2000a), CDI is modulated by synthetic Ca^{2+} buffers (EGTA, BAPTA) and by the Ca^{2+} buffers PV and CB-D28k in vitro (Kreiner and Lee 2005). Of note, PV and CB-D28k affect $Ca_v2.1$ channel function differently than the synthetic buffers EGTA and BAPTA, often presumed to serve as close substitutes for endogenous Ca^{2+} buffers. CDI of $Ca_v2.1$ channel is assumed to depend on intracellular Ca^{2+} microdomains around Ca^{2+} channels. These microdomains are expected to be differently affected by various Ca^{2+} buffers, which in turn specifically influence the inactivation properties of the Ca^{2+} channels. Contrary to the expectation based on in vitro experiments, CDI in Purkinje cells of double knockout (CB-D28k$^{-/-}$PV$^{-/-}$) mice is not increased. However, P-type currents recorded in these cells exhibit increased voltage-dependent inactivation as the result of a decreased expression of the auxiliary $Ca_v\beta2a$ subunit compared to WT neurons (Kreiner et al. 2010) (Fig. 2). This, together with the observation that spontaneous action potentials are not different in CB-D28k$^{-/-}$PV$^{-/-}$ and WT Purkinje cells, indicates that increased inactivation due to molecular switching of $Ca_v2.1$ beta subunits may preserve normal activity-dependent Ca^{2+} signals in the absence of PV and CB-D28k.

A cross talk between the regulation of a Ca^{2+} channel and Ca^{2+} buffer expression in Purkinje cells is also observed in leaner mice that have a mutation in the pore-forming alpha subunit of $Ca_v2.1$. The strongly-reduced $Ca_v2.1$ Ca^{2+} channel function leads to adaptive changes consisting of a diminished rapid Ca^{2+} buffering/

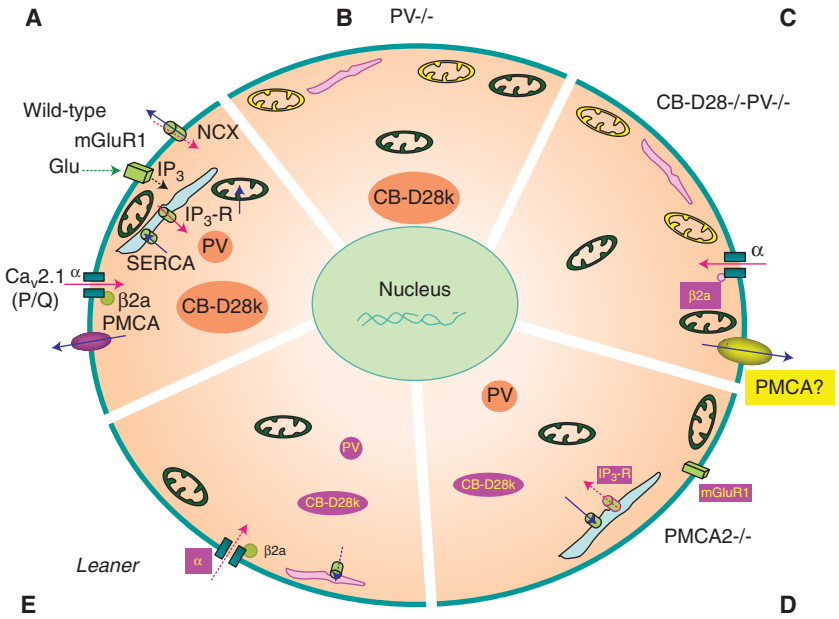

Figure 2. Homeostatic/adaptive changes in the soma of Purkinje cells (PC) caused by malfunctioning or elimination of Ca^{2+}-signaling toolkit component(s); regulation by the Ca^{2+} homeostasome. (*A*) A detailed situation is depicted for wild-type mice. Increases in $[Ca^{2+}]_i$ (red arrows) result from influx via $Ca_V2.1$ (P/Q) channels or release from internal stores (light blue) via the IP_3 receptor. IP_3 is generated by the activation of metabotropic glutamate receptors (mGluR). Ca^{2+} removal systems (blue arrows) include PMCA and NCX in the plasma membrane, SERCA pumps, and mitochondria (green). Identified Ca^{2+}-signaling toolkit components including organelles, which are up- or down-regulated, are marked in yellow and magenta, respectively. (*B*) In $PV^{-/-}$, PC subplasmalemmal mitochondria are increased, while ER volume directly underneath the plasma membrane is decreased. (*C*) In addition to the changes observed in $PV^{-/-}$, in PC lacking both, PV and CB-D28k the auxiliary $Ca_V\beta2a$ subunit of $Ca_V2.1$ (P/Q), is decreased, leading to increased voltage-dependent inactivation of P-type currents. Model studies indicate an up-regulation of Ca^{2+} extrusion systems, possibly PMCA. (*D*) In $PMCA2^{-/-}$ PC, expression of mGluR1 and of IP_3 receptor type 1 (IP3R1), responsible for the Ca^{2+} release from ER stores, is decreased. Also, the cytosolic Ca^{2+} buffering capacity mediated by CB-D28k is decreased. (*E*) In leaner mice PC that are characterized by strongly attenuated $Ca_V2.1$ Ca^{2+} channel function, the rapid Ca^{2+} buffering/sequestering capacity is reduced: PV and CB-D28k are down-regulated and (subplasmalemmal) ER is decreased/impaired, leading to reduced Ca^{2+} uptake.

sequestering capacity of Purkinje cells (Dove et al. 2000). The Ca^{2+} buffering capacity is less than 50% compared to Purkinje cells from WT mice, due to reduced PV and CB-D28k expression levels (Fig. 2). In addition, reduced Ca^{2+} uptake by the (likely subplasmalemmal) ER further contributes to the reduced buffering ability of leaner mice Purkinje cells (Murchison et al. 2002). Also, impairment of proteins responsible for Ca^{2+} extrusion in Purkinje cells activates the Ca^{2+} homeostasome. In Purkinje cells of mice with a mutation in PMCA2 characterized by a reduced Ca^{2+} extrusion, the rise in $[Ca^{2+}]_i$ during high K^+-induced depolarization is decreased. This is indicative of a Ca_v channel down-regulation likely to regulate $[Ca^{2+}]_i$ toward normal homeostasis (Ueno et al. 2002). $PMCA2^{-/-}$ mice have decreased expression levels of CB-D28k (Hu et al. 2006), metabotropic glutamate receptor 1 (mGluR1), and of $InsP_3$ receptor type 1 (IP3R1), responsible for the Ca^{2+} release from ER stores (Kurnellas et al. 2007) (Fig. 2). Again, this reduction in mGluR1-mediated $[Ca^{2+}]_i$ elevation may be viewed as an adaptive mechanism to cope with the reduced Ca^{2+} extrusion. The authors

suggest that "the decrease in the expression of mGluR1 and its downstream effectors and perturbations in the mGluR1-signaling complex in the absence of PMCA2 may cumulatively result in aberrant mGluR signaling in Purkinje neurons, leading to cerebellar deficits in the PMCA2-null mouse." However, the severely distorted PMCA2$^{-/-}$ Purkinje cell morphology (smaller cell body, distorted dendritic tree) may also be a likely cause for the ataxic phenotype (Empson et al. 2007). In addition to the identified changes occurring in Purkinje cells of CB-D28k$^{-/-}$PV$^{-/-}$ mice, an up-regulation of Ca^{2+} extrusion/uptake mechanisms was hypothesized, since the decay of dendritic Ca^{2+} signals could be accurately fitted only when applying a two-fold higher Ca^{2+} extrusion rate, compared to the rates sufficient to model the Ca^{2+} transients in PV$^{-/-}$ and WT Purkinje cells (Schmidt et al. 2003b). Currently, no experimental data is available to account for the increased dendritic $[Ca^{2+}]_i$ decay in CB-D28k$^{-/-}$PV$^{-/-}$ Purkinje cells; putative candidates are PMCA isoforms, NCX isoforms, or increased uptake into stores.

What are the evidences that the changes discussed above are not "simple" compensation mechanisms, but may be considered as "truly homeostatic" mechanisms? One argument is the generality of the mechanism and a second one the reciprocality as exemplified for the relationship between PV content and mitochondrial volume. In the absence of PV in PV$^{-/-}$ mice, an up-regulation of mitochondria occurs not only in PV-ergic Purkinje cells (Chen et al. 2006) or cerebellar stellate and basket cells (B Schwaller, unpubl.), but is also seen in PV$^{-/-}$ fast-twitch muscle fibers (Chen et al. 2001). The latter are characterized by high PV expression levels in WT mice. Vice versa, in transgenic mice ectopically expressing PV in striatal neurons (Van Den Bosch et al. 2002), a neuron subpopulation normally not expressing PV, the mitochondrial volume is decreased by almost 50% (Maetzler et al. 2004). This reduction accounts for the heightened excitotoxic injury provoked by a local injection of ibotenic acid. A last example of reciprocality: elimination of PV and CB-D28k from Purkinje cells alters $Ca_v2.1$ channel function (Kreiner et al. 2010), while a reduced Ca^{2+} influx due to a mutation in the $Ca_v2.1$ channel down-regulates PV and CB-D28k (Dove et al. 2000). The elucidation of the pathways and molecular mechanisms responsible for the regulation of the Ca^{2+} homeostasome remains an exciting topic for future research.

ACKNOWLEDGMENTS

I would like to thank Thomas Henzi and Walter-Vincent Blum, University of Fribourg, for helpful comments.

REFERENCES

Airaksinen L, Virkkala J, Aarnisalo A, Meyer M, Ylikoski J, Airaksinen MS. 2000. Lack of calbindin-D28k does not affect hearing level or survival of hair cells in acoustic trauma. *ORL J Otorhinolaryngol Relat Spec* **62:** 9–12.

Airaksinen MS, Eilers J, Garaschuk O, Thoenen H, Konnerth A, Meyer M. 1997. Ataxia and altered dendritic calcium signaling in mice carrying a targeted null mutation of the calbindin D28k gene. *Proc Natl Acad Sci U S A* **94:** 1488–1493.

Akke M, Forsen S, Chazin WJ. 1991. Molecular basis for co-operativity in Ca^{2+} binding to calbindin D9k. 1H nuclear magnetic resonance studies of (Cd^{2+})1-bovine calbindin D9k. *J Mol Biol* **220:** 173–189.

Allbritton NL, Meyer T, Stryer L. 1992. Range of messenger action of calcium ion and inositol 1,4,5,-trisphophate. *Science* **258:** 1812–1815.

Babini E, Bertini I, Capozzi F, Del Bianco C, Hollender D, Kiss T, Luchinat C, Quattrone A. 2004. Solution structure of human beta-parvalbumin and structural comparison with its paralog alpha-parvalbumin and with their rat orthologs. *Biochemistry* **43:** 16076–16085.

Baldellon C, Alattia JR, Strub MP, Pauls T, Berchtold MW, Cave A, Padilla A. 1998. N-15 NMR relaxation studies of calcium-loaded parvalbumin show tight dynamics compared to those of other EF-hand proteins. *Biochemistry* **37:** 9964–9975.

Barski JJ, Hartmann J, Rose CR, Hoebeek F, Morl K, Noll-Hussong M, De Zeeuw CI, Konnerth A, Meyer M. 2003. Calbindin in cerebellar Purkinje cells is a critical determinant of the precision of motor coordination. *J Neurosci* **23:** 3469–3477.

Bearzatto B, Servais L, Roussel C, Gall D, Baba-Aissa F, Schurmans S, de Kerchove d'Exaerde A, Cheron G, Schiffmann SN. 2006. Targeted calretinin expression in granule cells of calretinin-null mice restores normal cerebellar functions. *FASEB J* **20:** 380–382.

Bellido T, Huening M, Raval-Pandya M, Manolagas SC, Christakos S. 2000. Calbindin-D28k is expressed in osteoblastic cells and suppresses their apoptosis by inhibiting caspase-3 activity. *J Biol Chem* **275:** 26328–26332.

Berggard T, Miron S, Onnerfjord P, Thulin E, Akerfeldt KS, Enghild JJ, Akke M, Linse S. 2002a. Calbindin D28k exhibits properties characteristic of a Ca^{2+} sensor. *J Biol Chem* **277:** 16662–16672.

Berggard T, Szczepankiewicz O, Thulin E, Linse S. 2002b. Myo-inositol monophosphatase is an activated target of calbindin D28k. *J Biol Chem* **277:** 41954–41959.

Berridge MJ, Bootman MD, Roderick HL. 2003. Calcium signalling: dynamics, homeostasis and remodelling. *Nat Rev Mol Cell Biol* **4:** 517–529.

Billing-Marczak K, Kuznicki J. 1999. Calretinin–sensor or buffer–function still unclear. *Pol J Pharmacol* **51:** 173–178.

Billups B, Forsythe ID. 2002. Presynaptic mitochondrial calcium sequestration influences transmission at mammalian central synapses. *J Neurosci* **22:** 5840–5847.

Boitier E, Rea R, Duchen MR. 1999. Mitochondria exert a negative feedback on the propagation of intracellular Ca^{2+} waves in rat cortical astrocytes. *J Cell Biol* **145:** 795–808.

Bindels RJ, Hartog A, Timmermans JA, van Os CH. 1991a. Immunocytochemical localization of calbindin-D28k, calbindin-D9k and parvalbumin in rat kidney. *Contrib Nephrol* **91:** 7–13.

Bindels RJ, Timmermans JA, Hartog A, Coers W, van Os CH. 1991b. Calbindin-D9k and parvalbumin are exclusively located along basolateral membranes in rat distal nephron. *J Am Soc Nephrol* **2:** 1122–1129.

Bindreither D, Lackner P. 2009. Structural diversity of calcium binding sites. *Gen Physiol Biophys* **28:** F82–F88.

Blatow M, Caputi A, Burnashev N, Monyer H, Rozov A. 2003. Ca^{2+} buffer saturation underlies paired pulse facilitation in calbindin-D28k-containing terminals. *Neuron* **38:** 79–88.

Boros S, Bindels RJ, Hoenderop JG. 2009. Active Ca^{2+} reabsorption in the connecting tubule. *Pflugers Arch* **458:** 99–109.

Bucurenciu I, Kulik A, Schwaller B, Frotscher M, Jonas P. 2008. Nanodomain Coupling between Ca^{2+} Channels and Ca^{2+} Sensors Promotes Fast and Efficient Transmitter Release at a Cortical GABAergic Synapse. *Neuron* **57:** 536–545.

Caillard O, Moreno H, Schwaller B, Llano I, Celio MR, Marty A. 2000. Role of the calcium-binding protein parvalbumin in short-term synaptic plasticity. *Proc Natl Acad Sci U S A* **97:** 13372–13377.

Camacho P, Lechleiter JD. 1995. Calreticulin inhibits repetitive intracellular Ca^{2+} waves. *Cell* **82:** 765–771.

Cao LP, Bolt MJ, Wei M, Sitrin MD, Chun Li Y. 2002. Regulation of calbindin-D9k expression by 1,25-dihydroxyvitamin D(3) and parathyroid hormone in mouse primary renal tubular cells. *Arch Biochem Biophys* **400:** 118–124.

Carafoli E, Genazzani A, Guerini D. 1999. Calcium controls the transcription of its own transporters and channels in developing neurons. *Biochem Biophys Res Commun* **266:** 624–632.

Celio M, Pauls T, Schwaller B (ed.) 1996. *Guidebook to the Calcium-Binding Proteins*. Oxford University Press, Oxford.

Chen G, Carroll S, Racay P, Dick J, Pette D, Traub I, Vrbova G, Eggli P, Celio M, Schwaller B. 2001. Deficiency in parvalbumin increases fatigue resistance in fast-twitch muscle and upregulates mitochondria. *Am J Physiol (Cell Physiol)* **281:** C114–C122.

Chen G, Racay P, Bichet S, Celio MR, Eggli P, Schwaller B. 2006. Deficiency in parvalbumin, but not in calbindin D-28k upregulates mitochondrial volume and decreases smooth endoplasmic reticulum surface selectively in a peripheral, subplasmalemmal region in the soma of Purkinje cells. *Neuroscience* **142:** 97–105.

Cheron G, Gall D, Servais L, Dan B, Maex R, Schiffmann SN. 2004. Inactivation of calcium-binding protein genes induces 160 Hz oscillations in the cerebellar cortex of alert mice. *J Neurosci* **24:** 434–441.

Cheung WT, Richards DE, Rogers JH. 1993. Calcium binding by chick calretinin and rat calbindin D28k synthesised in bacteria. *Eur J Biochem* **215:** 401–410.

Chin D, Means AR. 2000. Calmodulin: a prototypical calcium sensor. *Trends Cell Biol* **10:** 322–328.

Choi KC, Jeung EB. 2008. Molecular mechanism of regulation of the calcium-binding protein calbindin-D(9k), and its physiological role(s) in mammals: a review of current research. *J Cell Mol Med* **12:** 409–420.

Christakos S, Dhawan P, Peng X, Obukhov AG, Nowycky MC, Benn BS, Zhong Y, Liu Y, Shen Q. 2007. New insights into the function and regulation of vitamin D target proteins. *J Steroid Biochem Mol Biol* **103:** 405–410.

Collin T, Chat M, Lucas MG, Moreno H, Racay P, Schwaller B, Marty A, Llano I. 2005. Developmental changes in parvalbumin regulate presynaptic Ca^{2+} signaling. *J Neurosci* **25:** 96–107.

Cox JA, Milos M, MacManus JP. 1990. Calcium- and magnesium-binding properties of oncomodulin. Direct binding studies and microcalorimetry. *J Biol Chem* **265:** 6633–6637.

Cox JA, Durussel I, Scott DJ, Berchtold MW. 1999. Remodeling of the AB site of rat parvalbumin and oncomodulin into a canonical EF-hand. *Eur J Biochem* **264:** 790–799.

Csillik B, Schwaller B, Mihaly A, Henzi T, Losonczic E, Knyihar-Csillik E. 2010. Upregulated expression of oncomodulin, the beta isoform of parvalbumin, in perikarya and axons in the diencephalon of parvalbumin knockout mice. *Neuroscience* **165:** 749–757.

D'Orlando C, Fellay B, Schwaller B, Salicio V, Bloc A, Gotzos V, Celio MR. 2001. Calretinin and calbindin D-28k delay the onset of cell death after excitotoxic stimulation in transfected P19 cells. *Brain Res* **909:** 145–158.

Dargan SL, Schwaller B, Parker I. 2004. Spatiotemporal patterning of IP3-mediated Ca^{2+} signals in Xenopus oocytes by Ca^{2+}-binding proteins. *J Physiol* **556:** 447–461.

Darwish H, Krisinger J, Furlow JD, Smith C, Murdoch FE, DeLuca HF. 1991. An estrogen-responsive element mediates the transcriptional regulation of calbindin D-9K gene in rat uterus. *J Biol Chem* **266:** 551–558.

de Solages C, Szapiro G, Brunel N, Hakim V, Isope P, Buisseret P, Rousseau C, Barbour B, Lena C. 2008. High-frequency organization and synchrony of activity in the purkinje cell layer of the cerebellum. *Neuron* **58:** 775–788.

Dove LS, Nahm SS, Murchison D, Abbott LC, Griffith WH. 2000. Altered calcium homeostasis in cerebellar Purkinje cells of leaner mutant mice. *J Neurophysiol* **84:** 513–524.

Eberhard M, Erne P. 1994. Calcium and magnesium binding to rat parvalbumin. *Eur J Biochem* **222:** 21–26.

Edmonds B, Reyes R, Schwaller B, Roberts WM. 2000. Calretinin modifies presynaptic calcium signaling in frog saccular hair cells. *Nat Neurosci* **3:** 786–790.

Empson RM, Garside ML, Knopfel T. 2007. Plasma membrane Ca^{2+} ATPase 2 contributes to short-term synapse plasticity at the parallel fiber to Purkinje neuron synapse. *J Neurosci* **27:** 3753–3758.

Faas GC, Schwaller B, Vergara JL, Mody I. 2007. Resolving the fast kinetics of cooperative binding: Ca^{2+} buffering by calretinin. *PLoS Biol* **5:** e311. doi: 310.1371/journal.pbio.0050311.

Farre-Castany MA, Schwaller B, Gregory P, Barski J, Mariethoz C, Eriksson JL, Tetko IV, Wolfer D, Celio MR, Schmutz I, Albrecht U, Villa AE. 2007. Differences in locomotor behavior revealed in mice deficient for the calcium-binding proteins parvalbumin, calbindin D-28k or both. *Behav Brain Res* **178:** 250–261.

Feher JJ. 1984. Measurement of facilitated calcium diffusion by a soluble calcium-binding protein. *Biochim Biophys Acta* **773:** 91–98.

Fierro L, Llano I. 1996. High endogenous calcium buffering in Purkinje cells from rat cerebellar slices. *J Physiol* **496:** 617–625.

Finn BE, Kordel J, Thulin E, Sellers P, Forsen S. 1992. Dissection of calbindin D9k into two Ca^{2+}-binding subdomains by a combination of mutagenesis and chemical cleavage. *FEBS Lett* **298:** 211–214.

Freund TF. 2003. Interneuron Diversity series: Rhythm and mood in perisomatic inhibition. *Trends Neurosci* **26:** 489–495.

Gabso M, Neher E, Spira ME. 1997. Low mobility of the Ca^{2+} buffers in axons of cultured Aplysia neurons. *Neuron* **18:** 473–481.

Gall D, Roussel C, Susa I, D'Angelo E, Rossi P, Bearzatto B, Galas MC, Blum D, Schurmans S, Schiffmann SN. 2003. Altered neuronal excitability in cerebellar granule cells of mice lacking calretinin. *J Neurosci* **23:** 9320–9327.

Gifford JL, Walsh MP, Vogel HJ. 2007. Structures and metal-ion-binding properties of the Ca^{2+}-binding helix-loop-helix EF-hand motifs. *Biochem J* **405:** 199–221.

Gurden H, Schiffmann SN, Lemaire M, Bohme GA, Parmentier M, Schurmans S. 1998. Calretinin expression as a critical component in the control of dentate gyrus long-term potentiation induction in mice. *Eur J Neurosci* **10:** 3029–3033.

Hackney CM, Mahendrasingam S, Penn A, Fettiplace R. 2005. The concentrations of calcium buffering proteins in mammalian cochlear hair cells. *J Neurosci* **25:** 7867–7875.

Hauk TG, Muller A, Lee J, Schwendener R, Fischer D. 2008. Neuroprotective and axon growth promoting effects of intraocular inflammation do not depend on oncomodulin or the presence of large numbers of activated macrophages. *Exp Neurol* **209:** 469–482.

Heizmann CW, Berchtold MW, Rowlerson AM. 1982. Correlation of parvalbumin concentration with relaxation speed in mammalian muscles. *Proc Natl Acad Sci U S A* **79:** 7243–7247.

Henzl MT, Tanner JJ. 2007. Solution structure of Ca^{2+}-free rat beta-parvalbumin (oncomodulin). *Protein Sci* **16:** 1914–1926.

Henzl MT, Tanner JJ. 2008. Solution structure of Ca^{2+}-free rat alpha-parvalbumin. *Protein Sci* **17:** 431–438.

Hu J, Qian J, Borisov O, Pan S, Li Y, Liu T, Deng L, Wannemacher K, Kurnellas M, Patterson C, Elkabes S, Li H. 2006. Optimized proteomic analysis of a mouse model of cerebellar dysfunction using amine-specific isobaric tags. *Proteomics* **6:** 4321–4334.

Huybers S, Naber TH, Bindels RJ, Hoenderop JG. 2007. Prednisolone-induced Ca^{2+} malabsorption is caused by diminished expression of the epithelial Ca^{2+} channel TRPV6. *Am J Physiol Gastrointest Liver Physiol* **292:** G92–G97.

Jouaville LS, Ichas F, Holmuhamedov EL, Camacho P, Lechleiter JD. 1995. Synchronization of calcium waves by mitochondrial substrates in Xenopus laevis oocytes. *Nature* **377:** 438–441.

Kallfelz FA, Taylor AN, Wasserman RH. 1967. Vitamin D-induced calcium binding factor in rat intestinal mucosa. *Proc Soc Exp Biol Med* **125:** 54–58.

Kang JS, Tian JH, Pan PY, Zald P, Li C, Deng C, Sheng ZH. 2008. Docking of axonal mitochondria by syntaphilin controls their mobility and affects short-term facilitation. *Cell* **132:** 137–148.

Kim MH, Korogod N, Schneggenburger R, Ho WK, Lee SH. 2005. Interplay between Na^{+}/Ca^{2+} exchangers and mitochondria in Ca^{2+} clearance at the calyx of Held. *J Neurosci* **25:** 6057–6065.

Klapstein GJ, Vietla S, Lieberman DN, Gray PA, Airaksinen MS, Thoenen H, Meyer M, Mody I. 1998. Calbindin-D28k fails to protect hippocampal neurons against ischemia in spite of its cytoplasmic calcium buffering properties: evidence from calbindin-D28k knockout mice. *Neuroscience* **85:** 361–373.

Kojetin DJ, Venters RA, Kordys DR, Thompson RJ, Kumar R, Cavanagh J. 2006. Structure, binding interface and hydrophobic transitions of Ca^{2+}-loaded calbindin-D(28K). *Nat Struct Mol Biol* **13:** 641–647.

Kordel J, Skelton NJ, Akke M, Chazin WJ. 1993. High-resolution structure of calcium-loaded calbindin D9k. *J Mol Biol* **231:** 711–734.

Kreiner L, Lee A. 2005. Endogenous and exogenous Ca^{2+} buffers differentially modulate Ca^{2+}-dependent inactivation of $Ca_V2.1$ Ca^{2+} channels. *J Biol Chem* **281:** 4691–4698.

Kreiner L, Christel CJ, Benveniste M, Schwaller B, Lee A. 2010. Compensatory regulation of Cav2.1 Ca^{2+} channels in cerebellar Purkinje neurons lacking parvalbumin and calbindin D-28k. *J Neurophysiol* **103:** 371–381.

Kretsinger RH, Nockolds CE. 1973. Carp muscle calcium-binding protein. II. Structure determination and general description. *J Biol Chem* **248:** 3313–3326.

Kurnellas MP, Lee AK, Li H, Deng L, Ehrlich DJ, Elkabes S. 2007. Molecular alterations in the cerebellum of the plasma membrane calcium ATPase 2 (PMCA2)-null mouse indicate abnormalities in Purkinje neurons. *Mol Cell Neurosci* **34:** 178–188.

Lambers TT, Mahieu F, Oancea E, Hoofd L, de Lange F, Mensenkamp AR, Voets T, Nilius B, Clapham DE,

Hoenderop JG, Bindels RJ. 2006. Calbindin-D28K dynamically controls TRPV5-mediated Ca^{2+} transport. *Embo J* **25:** 2978–2988.

Lee A, Scheuer T, Catterall WA. 2000a. Ca^{2+}/calmodulin-dependent facilitation and inactivation of P/Q-type Ca^{2+} channels. *J Neurosci* **20:** 6830–6838.

Lee GS, Choi KC, Jeung EB. 2006. Glucocorticoids differentially regulate expression of duodenal and renal calbindin-D9k through glucocorticoid receptor-mediated pathway in mouse model. *Am J Physiol Endocrinol Metab* **290:** E299–E307.

Lee SH, Rosenmund C, Schwaller B, Neher E. 2000b. Differences in Ca^{2+} buffering properties between excitatory and inhibitory hippocampal neurons from the rat. *J Physiol* **525:** 405–418.

Lee SH, Schwaller B, Neher E. 2000c. Kinetics of Ca^{2+} binding to parvalbumin in bovine chromaffin cells: implications for [Ca^{2+}] transients of neuronal dendrites. *J Physiol* **525:** 419–432.

Linse S, Johansson C, Brodin P, Grundstrom T, Drakenberg T, Forsen S. 1991. Electrostatic contributions to the binding of Ca^{2+} in calbindin D9k. *Biochemistry* **30:** 154–162.

Lips MB, Keller BU. 1998. Endogenous calcium buffering in motoneurones of the nucleus hypoglossus from mouse. *J Physiol (Lond)* **511:** 105–117.

Lukas W, Jones KA. 1994. Cortical neurons containing calretinin are selectively resistant to calcium overload and excitotoxicity. *Neuroscience* **61:** 307–316.

Lutz W, Frank EM, Craig TA, Thompson R, Venters RA, Kojetin D, Cavanagh J, Kumar R. 2003. Calbindin D28K interacts with Ran-binding protein M: identification of interacting domains by NMR spectroscopy. *Biochem Biophys Res Commun* **303:** 1186–1192.

Maeda H, Ellis-Davies GC, Ito K, Miyashita Y, Kasai H. 1999. Supralinear Ca^{2+} signaling by cooperative and mobile Ca^{2+} buffering in Purkinje neurons. *Neuron* **24:** 989–1002.

Maetzler W, Nitsch C, Bendfeldt K, Racay P, Vollenweider F, Schwaller B. 2004. Ectopic parvalbumin expression in mouse forebrain neurons increases excitotoxic injury provoked by ibotenic acid injection into the striatum. *Exp Neurol* **186:** 78–88.

Maki M, Kitaura Y, Satoh H, Ohkouchi S, Shibata H. 2002. Structures, functions and molecular evolution of the penta-EF-hand Ca^{2+}-binding proteins. *Biochim Biophys Acta* **1600:** 51–60.

Marenholz I, Heizmann CW, Fritz G. 2004. S100 proteins in mouse and man: from evolution to function and pathology (including an update of the nomenclature). *Biochem Biophys Res Commun* **322:** 1111–1122.

Marsden BJ, Shaw GS, Sykes BD. 1990. Calcium binding proteins. Elucidating the contributions to calcium affinity from an analysis of species variants and peptide fragments. *Biochem Cell Biol* **68:** 587–601.

Martin SR, Linse S, Johansson C, Bayley PM, Forsen S. 1990. Protein surface charges and Ca^{2+} binding to individual sites in calbindin D9k: stopped-flow studies. *Biochemistry* **29:** 4188–4193.

Maughan DW, Godt RE. 1999. Parvalbumin concentration and diffusion coefficient in frog myoplasm. *J Muscle Res Cell Motil* **20:** 199–209.

McLaughlin S, Mulrine N, Gresalfi T, Vaio G, McLaughlin A. 1981. Adsorption of divalent cations to bilayer membranes containing phosphatidylserine. *J Gen Physiol* **77:** 445–473.

Mihaly A, Szente M, Dubravcsik Z, Boda B, Kiraly E, Nagy T, Domonkos A. 1997. Parvalbumin- and calbindin-containing neurons express c-fos protein in primary and secondary (mirror) epileptic foci of the rat neocortex. *Brain Res* **761:** 135–145.

Moreland JL, Gramada A, Buzko OV, Zhang Q, Bourne PE. 2005. The Molecular Biology Toolkit (MBT): A Modular Platform for Developing Molecular Visualization Applications. *BMC Bioinformatics* **6:**21.

Morgan DW, Welton AF, Heick AE, Christakos S. 1986. Specific in vitro activation of Ca,Mg-ATPase by vitamin D-dependent rat renal calcium binding protein (calbindin D28K). *Biochem Biophys Res Commun* **138:** 547–553.

Muller A, Kukley M, Stausberg P, Beck H, Muller W, Dietrich D. 2005. Endogenous Ca^{2+} buffer concentration and Ca^{2+} microdomains in hippocampal neurons. *J Neurosci* **25:** 558–565.

Muller M, Felmy F, Schwaller B, Schneggenburger R. 2007. Parvalbumin is a mobile presynaptic Ca^{2+} buffer in the calyx of held that accelerates the decay of Ca^{2+} and short-term facilitation. *J Neurosci* **27:** 2261–2271.

Muntener M, Kaser L, Weber J, Berchtold MW. 1995. Increase of skeletal muscle relaxation speed by direct injection of parvalbumin cDNA. *Proc Natl Acad Sci U S A* **92:** 6504–6508.

Murchison D, Griffith WH. 2000. Mitochondria buffer nontoxic calcium loads and release calcium through the mitochondrial permeability transition pore and sodium/calcium exchanger in rat basal forebrain neurons. *Brain Res* **854:** 139–151.

Murchison D, Dove LS, Abbott LC, Griffith WH. 2002. Homeostatic compensation maintains Ca^{2+} signaling functions in Purkinje neurons in the leaner mutant mouse. *Cerebellum* **1:** 119–127.

Nagerl UV, Mody I. 1998. Calcium-dependent inactivation of high-threshold calcium currents in human dentate gyrus granule cells. *J Physiol* **509:** 39–45.

Nagerl UV, Novo D, Mody I, Vergara JL. 2000. Binding kinetics of calbindin-D(28k) determined by flash photolysis of caged Ca^{2+}. *Biophys J* **79:** 3009–3018.

Neher E. 1998. Usefulness and limitations of linear approximations to the understanding of Ca^{2+} signals. *Cell Calcium* **24:** 345–357.

Nelson MR, Thulin E, Fagan PA, Forsen S, Chazin WJ. 2002. The EF-hand domain: a globally cooperative structural unit. *Protein Sci* **11:** 198–205.

Orduz D, Llano I. 2007. Recurrent axon collaterals underlie facilitating synapses between cerebellar Purkinje cells. *Proc Natl Acad Sci U S A* **104:** 17831–17836.

Palczewska M, Groves P, Ambrus A, Kaleta A, Kover KE, Batta G, Kuznicki J. 2001. Structural and biochemical characterization of neuronal calretinin domain I-II (residues 1–100). Comparison to homologous calbindin D28k domain I-II (residues 1–93). *Eur J Biochem* **268:** 6229–6237.

Pike CJ, Cotman CW. 1995. Calretinin-immunoreactivity neurons are resistant to B-amyloid toxicity in vitro. *Brain Res* **671:** 293–298.

Raymackers JM, Gailly P, Schoor MC, Pette D, Schwaller B, Hunziker W, Celio MR, Gillis JM. 2000. Tetanus relaxation of fast skeletal muscles of the mouse made parvalbumin deficient by gene inactivation. *J Physiol* **527:** 355–364.

Reddy D, Pollock AS, Clark SA, Sooy K, Vasavada RC, Stewart AF, Honeyman T, Christakos S. 1997. Transfection and overexpression of the calcium binding protein calbindin-D28k results in a stimulatory effect on insulin synthesis in a rat beta cell line (RIN 1046–38). *Proc Natl Acad Sci U S A* **94:** 1961–1966.

Reisner PD, Christakos S, Vanaman TC. 1992. In vitro enzyme activation with calbindin-D28k, the vitamin D-dependent 28 kDa calcium binding protein. *FEBS Lett* **297:** 127–131.

Rimessi A, Giorgi C, Pinton P, Rizzuto R. 2008. The versatility of mitochondrial calcium signals: from stimulation of cell metabolism to induction of cell death. *Biochim Biophys Acta* **1777:** 808–816.

Rodenbaugh DW, Wang W, Davis J, Edwards T, Potter JD, Metzger JM. 2007. Parvalbumin isoforms differentially accelerate cardiac myocyte relaxation kinetics in an animal model of diastolic dysfunction. *Am J Physiol Heart Circ Physiol* **293:** H1705–H1713.

Sabatini BL, Oertner TG, Svoboda K. 2002. The life cycle of Ca^{2+} ions in dendritic spines. *Neuron* **33:** 439–452.

Sakaguchi N, Henzl MT, Thalmann I, Thalmann R, Schulte BA. 1998. Oncomodulin is expressed exclusively by outer hair cells in the organ of Corti. *J Histochem Cytochem* **46:** 29–40.

Schiffmann SN, Cheron G, Lohof A, d'Alcantara P, Meyer M, Parmentier M, Schurmans S. 1999. Impaired motor coordination and Purkinje cell excitability in mice lacking calretinin. *Proc Natl Acad Sci U S A* **96:** 5257–5262.

Schmidt H, Brown EB, Schwaller B, Eilers J. 2003a. Diffusional mobility of parvalbumin in spiny dendrites of cerebellar purkinje neurons quantified by fluorescence recovery after photobleaching. *Biophys J* **84:** 2599–2608.

Schmidt H, Stiefel KM, Racay P, Schwaller B, Eilers J. 2003b. Mutational analysis of dendritic Ca^{2+} kinetics in rodent Purkinje cells: role of parvalbumin and calbindin D28k. *J Physiol* **551:** 13–32.

Schmidt H, Schwaller B, Eilers J. 2005. Calbindin D28k targets myo-inositol monophosphatase in spines and dendrites of cerebellar Purkinje neurons. *Proc Natl Acad Sci U S A* **102:** 5850–5855.

Schmidt H, Arendt O, Brown EB, Schwaller B, Eilers J. 2007a. Parvalbumin is freely mobile in axons, somata and nuclei of cerebellar Purkinje neurones. *J Neurochem* **100:** 727–735.

Schmidt H, Kunerth S, Wilms C, Strotmann R, Eilers J. 2007b. Spino-dendritic cross-talk in rodent Purkinje neurons mediated by endogenous Ca^{2+}-binding proteins. *J Physiol* **581:** 619–629.

Schmidt H, Eilers J. 2009. Spine neck geometry determines spino-dendritic cross-talk in the presence of mobile endogenous calcium binding proteins. *J Comput Neurosci* **27:** 229–243.

Schurmans S, Schiffmann SN, Gurden H, Lemaire M, Lipp H-P, Schwam V, Pochet R, Imperato A, Böhme GA, Parmentier M. 1997. Impaired LTP induction in the dentate gyrus of calretinin-deficient mice. *Proc. Natl. Acad. Sci.* **94:** 10415–10420.

Schwaller B, Durussel I, Jermann D, Herrmann B, Cox JA. 1997. Comparison of the Ca^{2+}-binding properties of human recombinant calretinin-22k and calretinin. *J Biol Chem* **272:** 29663–29671.

Schwaller B, Dick J, Dhoot G, Carroll S, Vrbova G, Nicotera P, Pette D, Wyss A, Bluethmann H, Hunziker W, Celio MR. 1999. Prolonged contraction-relaxation cycle of fast-twitch muscles in parvalbumin knockout mice. *Am J Physiol (Cell Physiol)* **276:** C395–403.

Schwaller B, Meyer M, Schiffmann S. 2002. 'New' functions for 'old' proteins: the role of the calcium-binding proteins calbindin D-28k, calretinin and parvalbumin, in cerebellar physiology. Studies with knockout mice. *Cerebellum* **1:** 241–258.

Schwaller B, Tetko IV, Tandon P, Silveira DC, Vreugdenhil M, Henzi T, Potier MC, Celio MR, Villa AE. 2004. Parvalbumin deficiency affects network properties resulting in increased susceptibility to epileptic seizures. *Mol Cell Neurosci* **25:** 650–663.

Schwaller B. 2007. Emerging Functions of the "Ca2+ Buffers" Parvalbumin, Calbindin D-28k and Calretinin in the Brain. In *Handbook of Neurochemistry and Molecular Neurobiology Neural Protein Metabolism and function* (ed. A Lajtha, N Banik), pp. 197–222. Springer, New York.

Schwaller B. 2009. The continuing disappearance of "pure" Ca^{2+} buffers. *Cell Mol Life Sci* **66:** 275–300.

Servais L, Bearzatto B, Schwaller B, Dumont M, De Saedeleer C, Dan B, Barski JJ, Schiffmann SN, Cheron G. 2005. Mono- and dual-frequency fast cerebellar oscillation in mice lacking parvalbumin and/or calbindin D-28k. *Eur J Neurosci* **22:** 861–870.

Skelton NJ, Kördel J, Akke M, Forsén S, Chazin WJ. 1994. Signal transduction versus buffering activity in Ca++-binding proteins. *Nat Struct Biol* **1:** 239–245.

Sooy K, Schermerhorn T, Noda M, Surana M, Rhoten WB, Meyer M, Fleischer N, Sharp GW, Christakos S. 1999. Calbindin-D(28k) controls $[Ca^{2+}]_i$ and insulin release. Evidence obtained from calbindin-d(28k) knockout mice and beta cell lines. *J Biol Chem* **274:** 34343–34349.

Stevens J, Rogers JH. 1997. Chick calretinin: purification, composition, and metal binding activity of native and recombinant forms. *Protein Expr Purif* **9:** 171–181.

Swain AL, Kretsinger RH, Amma EL. 1989. Restrained least squares refinement of native (calcium) and cadmium-substituted carp parvalbumin using X-ray crystallographic data at 1.6-A resolution. *J Biol Chem* **264:** 16620–16628.

Szabadkai G, Duchen MR. 2008. Mitochondria: the hub of cellular Ca^{2+} signaling. *Physiology* **23:** 84–94.

Szatkowski ML, Westfall MV, Gomez CA, Wahr PA, Michele DE, DelloRusso C, Turner II, Hong KE, Albayya FP, Metzger JM. 2001. In vivo acceleration of heart relaxation performance by parvalbumin gene delivery. *J Clin Invest* **107:** 191–198.

Tang Y, Zucker RS. 1997. Mitochondrial involvement in post-tetanic potentiation of synaptic transmission. *Neuron* **18:** 483–491.

Thalmann I, Shibasaki O, Comegys TH, Henzl MT, Senarita M, Thalmann R. 1995. Detection of a beta-parvalbumin isoform in the mammalian inner ear. *Biochem Biophys Res Commun* **215:** 142–147.

Tikunov BA, Rome LC. 2009. Is high concentration of parvalbumin a requirement for superfast relaxation? *J Muscle Res Cell Motil* **30:** 57–65.

Ueno T, Kameyama K, Hirata M, Ogawa M, Hatsuse H, Takagaki Y, Ohmura M, Osawa N, Kudo Y. 2002. A mouse with a point mutation in plasma membrane Ca^{2+}-ATPase isoform 2 gene showed the reduced Ca^{2+} influx in cerebellar neurons. *Neurosci Res* **42:** 287–297.

Van Den Bosch L, Schwaller B, Vleminckx V, Meijers B, Stork S, Ruehlicke T, Van Houtte E, Klaassen H, Celio MR, Missiaen L, Robberecht W, Berchtold MW. 2002. Protective effect of parvalbumin on excitotoxic motor neuron death. *Exp Neurol* **174:** 150–161.

Vecellio M, Schwaller B, Meyer M, Hunziker W, Celio MR. 2000. Alterations in Purkinje cell spines of calbindin D-28 k and parvalbumin knock-out mice. *Eur J Neurosci* **12:** 945–954.

Vreugdenhil M, Jefferys JG, Celio MR, Schwaller B. 2003. Parvalbumin-deficiency facilitates repetitive IPSCs and gamma oscillations in the hippocampus. *J Neurophysiol* **89:** 1414–1422.

Wang W, Metzger JM. 2008. Parvalbumin isoforms for enhancing cardiac diastolic function. *Cell Biochem Biophys* **51:** 1–8.

Wassle H, Peichl L, Airaksinen MS, Meyer M. 1998. Calcium-binding proteins in the retina of a calbindin-null mutant mouse. *Cell Tissue Res* **292:** 211–218.

Yin Y, Henzl MT, Lorber B, Nakazawa T, Thomas TT, Jiang F, Langer R, Benowitz LI. 2006. Oncomodulin is a macrophage-derived signal for axon regeneration in retinal ganglion cells. *Nat Neurosci* **9:** 843–852.

Zheng W, Xie Y, Li G, Kong J, Feng JQ, Li YC. 2004. Critical role of calbindin-D28k in calcium homeostasis revealed by mice lacking both vitamin D receptor and calbindin-D28k. *J Biol Chem* **279:** 52406–52413.

Zhou Z, Neher E. 1993. Mobile and immobile calcium buffers in bovine adrenal chromaffin cells. *J Physiol* **469:** 245–273.

Cold Spring Harbor Perspectives in Biology

Cytosolic Ca^{2+} Buffers

Beat Schwaller

Cold Spring Harb Perspect Biol published online October 13, 2010

Subject Collection Calcium Signaling

For additional articles in this collection, see http://cshperspectives.cshlp.org/cgi/collection/